

Mutations in *Cypher/ZASP* in Patients With Dilated Cardiomyopathy and Left Ventricular Non-Compaction

Matteo Vatta, PhD,* Bhagyalaxmi Mohapatra, PhD,* Shinawe Jimenez, MD,* Ximena Sanchez, PhD,* Georgine Faulkner, PhD,‡ Zeev Perles, MD,* Gianfranco Sinagra, MD,§ Juann-Huey Lin, MD,* Thuy M. Vu, BS,* Qiang Zhou, PhD,|| Karla R. Bowles, PhD,* Andrea Di Lenarda, MD,§ Lisa Schimmenti, MD,¶ Michelle Fox, MS,|| Michelle A. Chrisco, BS,* Ross T. Murphy, MD,# William McKenna, MD,# Perry Elliott, MD,# Neil E. Bowles, PhD,* Ju Chen, PhD,|| Giorgio Valle, PhD,** Jeffrey A. Towbin, MD, FACC*†

Houston, Texas; Trieste and Padova, Italy; La Jolla and Los Angeles, California; and London, United Kingdom

OBJECTIVES	We evaluated the role of <i>Cypher/ZASP</i> in the pathogenesis of dilated cardiomyopathy (DCM) with or without isolated non-compaction of the left ventricular myocardium (INLVM).
BACKGROUND	Dilated cardiomyopathy, characterized by left ventricular dilation and systolic dysfunction with signs of heart failure, is genetically transmitted in 30% to 40% of cases. Genetic heterogeneity has been identified with mutations in multiple cytoskeletal and sarcomeric genes causing the phenotype. In addition, INLVM with a hypertrophic dilated left ventricle, ventricular dysfunction, and deep trabeculations, is also inherited, and the genes identified to date differ from those causing DCM. <i>Cypher/ZASP</i> is a newly identified gene encoding a protein that is a component of the Z-line in both skeletal and cardiac muscle.
METHODS	Diagnosis of DCM was performed by echocardiogram, electrocardiogram, and physical examination. In addition, levels of the muscular isoform of creatine kinase were measured to evaluate for skeletal muscle involvement. <i>Cypher/ZASP</i> was screened by denaturing high performance liquid chromatography (DHPLC) and direct deoxyribonucleic acid sequencing.
RESULTS	We identified and screened 100 probands with left ventricular dysfunction. Five mutations in six probands (6% of cases) were identified in patients with familial or sporadic DCM or INLVM. In vitro studies showed cytoskeleton disarray in cells transfected with mutated <i>Cypher/ZASP</i> .
CONCLUSIONS	These data suggest that mutated <i>Cypher/ZASP</i> can cause DCM and INLVM and identify a mechanistic basis. (J Am Coll Cardiol 2003;42:2014–27) © 2003 by the American College of Cardiology Foundation

Dilated cardiomyopathy (DCM) is a primary heart muscle disease characterized by left ventricular dilation, systolic dysfunction, secondary diastolic dysfunction, and is occasionally associated right ventricular disease (1). A major cause of morbidity and mortality, DCM is the most common cause of congestive heart failure. This disorder affects

40 in every 100,000 of the population (2), often necessitating cardiac transplantation, with an estimated cost of \$10 to \$40 billion yearly in the U.S. (2). Depending on the diagnostic criteria used, the annual incidence ranges from 5 to 8 cases per 100,000 population (2,3), but the true incidence is probably higher as many asymptomatic cases go unrecognized.

The underlying causes of DCM are heterogeneous (4,5), including myocarditis, alcohol abuse, drug toxicity (such as adriamycin), and ischemia-induced, metabolic, and genetic abnormalities. In 30% to 40% of cases (6–8), DCM is a familial disease with a high level of heterogeneity. Autosomal dominant inheritance of DCM is the most common (5), with two main forms described as: 1) “pure” DCM, and 2) DCM associated with cardiac conduction system disease (CDDC) (9). Multiple genetic loci have been identified for autosomal dominant DCM, with mutations being identified in actin (10), desmin (11), lamin A/C (12), δ -sarcoglycan (13), β -sarcoglycan (14), β -myosin heavy chain (15), cardiac troponin T (15), α -tropomyosin (16), titin (17,18), vinculin (19), muscle LIM protein (20), and phospholamban (21,22). In addition, mutations in taffazzin (*G4.5*) cause DCM with endocardial fibroelastosis in patients with the Barth syndrome (23) or isolated non-compaction of the left

From the Departments of *Pediatrics (Cardiology) and †Molecular and Human Genetics, Baylor College of Medicine, Houston, Texas; ‡International Centre for Genetic Engineering and Biotechnology, Trieste, Italy; §Department of Cardiology, Ospedale Maggiore, Trieste, Italy; ||Institute of Molecular Medicine and Department of Medicine, University of California at San Diego, School of Medicine, La Jolla, California; ¶Department of Pediatrics (Genetics), University of California at Los Angeles, Los Angeles, California; #Department of Cardiological Sciences, St. George's Hospital Medical School, London, United Kingdom; and the **CRIBI Biotechnology Centre, Università degli Studi di Padova, Padova, Italy. This work was funded by grants from the International Society for Heart and Lung Transplantation (Dr. Vatta), the American Heart Association (Dr. Bowles), the Muscular Dystrophy Association (Drs. Towbin, Bowles, and Chen), the National Institutes of Health, National Heart, Lung, and Blood Institute (Dr. Towbin: R01-HL62570 and PO1 HL67155; Dr. Chen: 1R01-HL66100), and the John Patrick Albright Foundation (Dr. Towbin). Dr. Towbin is also supported by the Texas Children's Hospital Foundation Chair in Pediatric Cardiovascular Research, the Abercrombie Pediatric Cardiology Fund of Texas Children's Hospital, and contributions from the Powers family. The financial support of Telethon-Italy to Dr. Faulkner (Grant 1278) and Dr. Valle (Grant B.57) is gratefully acknowledged. Drs. Vatta, Mohapatra, and Jimenez contributed equally to the work. Joel S. Karliner acted as Guest Editor for this paper.

Manuscript received July 15, 2003; revised manuscript received October 6, 2003, accepted October 9, 2003.

Abbreviations and Acronyms

BAC	= bacterial artificial chromosome
DCM	= dilated cardiomyopathy
DNA	= deoxyribonucleic acid
DHPLC	= denaturing high performance liquid chromatography
GFP	= green fluorescence protein
INLVM	= isolated non-compaction of the left ventricular myocardium
LVNC	= left ventricular non-compaction
MRI	= magnetic resonance imaging
mRNA	= messenger ribonucleic acid
NYHA	= New York Heart Association
PCR	= polymerase chain reaction
RNA	= ribonucleic acid
RT	= reverse transcription
SDS	= sodium dodecylsulfate

ventricular myocardium (INLVM) (24), a disorder in which a dilated hypertrophic left ventricle with poor systolic function and deep trabeculations is notable (25). This phenotype, which is also known as left ventricular non-compaction (LVNC), is thought to occur because of arrested myocardial development. It has been reported to occur in isolation (frequently due to *G4.5* mutations) or in association with congenital heart disease. In the latter case, mutations in α -dystrobrevin have been reported (24).

We have previously proposed that DCM results from mutations that affect elements of the cytoarchitecture that connect the extracellular matrix to the nucleus through the sarcolemma, the dystrophin-associated glycoprotein complex, dystrophin, the cytoskeleton, the contractile apparatus, and the intermediate filaments (26). This has been supported by the genes identified for human forms of DCM to date, as well as animal models. A novel gene within this pathway, shown to result in cardiomyopathy in knockout mice, is a Z-band complex-encoding gene called *Cypher* (27). The characterization of the human gene, known as the Z-band alternatively spliced PDZ-motif protein (*ZASP*) (28), and analysis for mutations in patients with DCM or LVNC are reported here.

METHODS

Patient evaluation. All patients were evaluated by physical examination (particularly focused on the cardiac and neuromuscular systems), chest radiography, electrocardiography, echocardiography, and magnetic resonance imaging (MRI). Left ventricular size and function were evaluated by M-mode and two-dimensional Doppler and color Doppler echocardiographic images, as previously described (13). Serum creatine kinase levels were measured to evaluate the patients for the presence of skeletal myopathy.

After informed consent, blood for lymphoblastoid cell line immortalization and deoxyribonucleic acid (DNA) extraction (13) was obtained, as regulated by the Baylor College of Medicine Institutional Review Board.

Characterization of *ZASP* genomic structure. The bacterial artificial chromosomes (BACs) encoding the *Cypher/ZASP* gene were identified by hybridization of a human BAC filter library (RPCI-11, Roswell Park Cancer Institute, Buffalo, New York) with overrun probes followed by direct DNA sequencing of BAC DNA, using an ABI 310 (Applied Biosystems, Foster City, California) and Big Dye Terminator chemistry, according to the manufacturer's instructions.

Denaturing high performance liquid chromatography (DHPLC) and DNA sequence analysis. Genomic DNA samples were amplified by polymerase chain reaction (PCR) using primers designed to amplify the *Cypher/ZASP* gene in an exon-by-exon manner (Table 1) and analyzed by DHPLC, using a WAVE DNA Fragment Analysis System (Transgenomic, Omaha, Nebraska), as previously described (29). When an abnormal DHPLC peak was detected, the genomic DNA was re-amplified, and the PCR product purified, using the QIAquick PCR Purification Kit (Qiagen, Stanford, California), and sequenced, using an ABI 3100 (Applied Biosystems) and Big Dye Terminator chemistry as described in the previous text.

Expression analysis. We investigated the cardiac expression in humans of *Cypher/ZASP* isoforms by reverse transcription (RT)-PCR from total human heart messenger ribonucleic acid (mRNA) (Clontech, Palo Alto, California). The RT was performed as previously described (13). The PCR was carried out using the following primers: exon 2F (5'-ATCACACCAGGCAGCAAGG-3') and exon 2R (5'-CTGCAGGGTGAGGCTCAAGT-3'), which amplify a 152 bp PCR product from all isoforms; exon 4F (5'-ACCTTTAGCCCTGCCTTCTC-3') and exon 4R (5'-AGGGTCTCTGCCGAGTACAG-3'), which generate a 200 bp product from *Cypher/ZASP4-6*; exon 10F (5'-CACCTGCTGCTGCCTCTC-3') and exon 10R (5'-GTCGGCAGGACTTGAAGC-3'), which generate a 110 bp PCR product from the *Cypher/ZASP2* and *-4* isoforms; exon 5F (5'-GTAGTCAACTCTCCAGCCA-3') and exon 6R (5'-ATGATGGCATCCTGGGAATA-3'), which amplify a 176 bp product from the *Cypher/ZASP1*, *-2*, and *-3* isoforms; and exon 7F (5'-AAGGACCTTGCCGTAGACAG-3') and exon 7R (5'-AATTCTGTCCCCGTCATCTG-3'), which amplify a 155 bp PCR product from all *Cypher/ZASP* isoforms. Primers to amplify the glucose-6-phosphate mRNA were used as positive controls (30), whereas RT reactions lacking reverse transcriptase were performed as negative controls.

The PCR was performed in a 30 μ l reaction containing 1.5 mmol/l $MgCl_2$, 10 pmol of each primer, 200 μ mol/l dNTP, and 0.5 U platinum *Taq* DNA polymerase (Invitrogen, Carlsbad, California), using a Stratagene Robocycler. Following a 5-min denaturation step at 94°C, 35 rounds of amplification (94°C for 30 s, 54°C to 60°C for 30 s, 72°C for 20 s) were performed. This was followed by a 72°C incubation for 2 min. The PCR products were analyzed by 2% agarose gel electrophoresis. All RT-PCR products were

Table 1. Primers Used for the Screening of the *Cypher/ZASP* Gene

Exon	Primer	Primer Sequence (5'-3')	T _A * (°C)	PCR Product Size (bp)
1	ZASP 1F	GTGCCCTCTCACTCAACCCCT	62	221
	ZASP 1R	ACACATGCCCTCCTCCAAGC		
2	ZASP 2F	TGGCCTTTCCTCAGGACCAC	56	335
	ZASP 2R	TCCTGCACAGTTTTGTAGCC		
3	ZASP 3F	TGACTCTGGCTCTCTTTGCT	54	230
	ZASP 3R	TCCAGGAACCAGGGCTGAGT		
4	ZASP 4F	GGCTCGCGCTAACACATCTG	58	506
	ZASP 4R	GCCACCTGTGGAGAGCTGTA		
5	ZASP 5F	CACTCCTTGCTCTCCTCACC	60	266
	ZASP 5R	CTCTATCCACGCCAGACACA		
6	ZASP 6F	TGTAACCGCCACCTGTTGCC	58	380
	ZASP 6R	TCCAGGAGGTCCAACGTGAG		
7	ZASP 7F	CCACCAATGGGCATGGAGCA	55	353
	ZASP 7R	AGCAGGACTCCCTGGCTTCT		
8	ZASP 8F	TTGCTGTGTCTCCCGTGAGT	56	178
	ZASP 8R	GAGGTCCCTTCCATGAGTGA		
9	ZASP 9F	GGTGAACACATTCCCTAACC	54	317
	ZASP 9R	CCCAGCAGAGTTATACATTG		
10	ZASP 10F	GCTCCCTTGACCTGTTGTCT	64	331
	ZASP 10R	GCCCTAACTACCTTGGACAC		
11	ZASP 11F	GGCTGTCCCTCTGGGTGTAA	54	257
	ZASP 11R	TCTTGGCTCTTGTGGCTCCT		
12A	ZASP 12AF	CATTTCTCTGGCTAGGAGTG	58	348
	ZASP 12AR	CTGGGAGAAGCTATCATCTG		
12B	ZASP 12BF	TGCACCCTCGGTGGCCTACA	58	352
	ZASP 12BR	CTCCAACCAGGGCTCAGAC		
13	ZASP 13F	GTCTGGGAGCTGCCTTACT	54	267
	ZASP 13R	GGAAGAGACATGGGTCAGAG		
14	ZASP 14F	AGTCAAGCCCGTCCCTCTC	55	200
	ZASP 14R	CACATGCCATCGAAGTGTTT		
15	ZASP 15F	TGATTTGGGGTTTGTCTTGG	53	290
	ZASP 15R	CTAGCGTGGCAAGGTATGTA		
16	ZASP 16F	GTCTCACGCAGGTCTGTTCT	53	229
	ZASP 16R	GCTTCCTCTCTCTCCCATT		

*T_A is the annealing temperature used in the polymerase chain reactions (PCR) reactions.

sequenced to confirm their identity, cloned in pCR2.1-TOPO (Invitrogen), and used as probes for Northern blot analysis (see the following text).

Northern blot analysis. A total of 15 µg of isolated total human heart ribonucleic acid (RNA) (Ambion, Austin, Texas) was denatured in a formamide/formaldehyde solution at 68°C for 10 min and samples were resolved on 1% denaturing agarose gel electrophoresis. The gel was stained with ethidium bromide solution and photographed; after washing, the RNA was transferred to a Hybond-N⁺ nylon membrane (Amersham Bioscience, Piscataway, New Jersey). After ultraviolet cross-linking, blots were pre-hybridized in a buffer containing 50 mmol/l piperazine-N,N'-bis (2-ethanesulfonic acid), 100 mmol/l NaCl, 50 mmol/l sodium phosphate (pH 7.0), 1 mmol/l ethylenediamine-tetraacetic acid, and 5% sodium dodecyl sulfate (SDS) at 55°C for 30 min. Cloned complementary DNA probes were radiolabeled with [α -³²P] deoxycytidine triphosphate (3,000 Ci/mmol) (Amersham Bioscience), and added to the pre-hybridization solution. The membranes were hybridized for 16 h at 65°C, then washed in 1×

standard saline citrate containing 5% SDS at 55°C for 30 min, and exposed to X-ray film at -80°C.

Site-directed mutagenesis. The *Cypher/ZASP* D117N mutant was prepared using the QuikChange Site-Directed Mutagenesis Kit (Stratagene, La Jolla, California) employing the plasmid plasmid cDNA 3.1(-)-*Cypher/ZASP*-WT, which contains the open reading frame of *Cypher/ZASP1* cloned into the *Bam*HI and *Hind*III restriction sites of the pcDNA 3.1(-) vector (Invitrogen), as a template. The following primers were used: 117-F (5'-CCAGCCAACGCCAAC-TACCAGGAACGC-3') and 117-R (5'-GCGTT-CCTGGTAGTTGGCGTTGGCTGG-3'). The PCR was performed with 10 ng of template DNA in a 50 µl reaction containing 200 nmol/l of each primer, 200 µmol/l of dNTP mix, 2.5 U of *Pfu*⁺ Turbo DNA polymerase (Stratagene), and 15 rounds of amplification (95°C for 30 s, 55°C for 1 min, 68°C for 12.5 min). Subsequently, the PCR product was incubated at 37°C for 1 h with 10 U of *Dpn* I, and 5 µl were used to transform XL1-blue Supercompetent cells (Invitrogen). The mutated *Cypher/ZASP* clones were sequenced to ensure the presence of the D117N mutation, as well as the

absence of other substitutions introduced by the DNA polymerase. The wild-type and mutated *Cypher/ZASP* inserts were then sub-cloned by PCR into the pcDNA 3.1/NT-GFP-TOPO vector (Invitrogen) and re-sequenced.

Mammalian cell transfection and immunohistochemistry. Transient transfections of the skeletal myoblast cell line C2C12 with the wild-type and mutant pcDNA 3.1(-)-*Cypher/ZASP* or pcDNA 3.1/NT-GFP-TOPO-*Cypher/ZASP* constructs were performed using Lipofectamine Plus (Invitrogen), according to the manufacturer's instructions. Cells were maintained in growth medium containing 10% fetal calf serum (Invitrogen) for 24 h post-transfection.

Cypher/ZASP-GFP fusion proteins were detected in transfected cells by washing with 1× phosphate-buffered saline, fixation with a 70% acetone:30% ethanol solution at -20°C for 30 min, followed by incubation for 45 min with 1.5 μmol/l tetra-rhodamine isothiocyanate-labeled phalloidin (Molecular Probes, Eugene, Oregon) and (4',6'-diamidino-2-phenylindole (Molecular Probes) for actin filament and nuclear staining, respectively, while green fluorescence protein (GFP) fluorescence was detected directly. Fluorescence was visualized as previously described (22,31).

Western blot analysis. The C2C12 cells transfected with wt-*Cypher/ZASP*, and D117N-*Cypher/ZASP* were harvested 24 h post-transfection and washed three times in phosphate-buffered saline. After sedimentation by centrifugation (1,000 × g, 5 min) the cells were soaked in 500 μl of hypotonic buffer (1 mmol/l NaHCO₂) containing 2 mmol/l phenylmethyl myeloid fluoride and 1 μg/ml of aprotinin, and lysed by three cycles of freeze and thaw. Proteins were separated into soluble and insoluble fraction by centrifugation at 15,000 g for 10 min. The supernatants were mixed with 0.5 volumes of 3× loading buffer (30% glycerol, 6% SDS, 62.5 mmol/l Tris-base-hydrochloric acid buffer, pH 6.8). The pellet was re-suspended in 750 μl of 1× loading buffer (10% glycerol, 2% SDS, 62.5 mmol/l Tris-base-hydrochloric acid buffer, pH 6.8) and then clarified by centrifugation at 15,000 g for 15 min.

After dilution in Laemmli sample buffer (Bio-Rad, Hercules, California) and heating to 100°C for 5 min, 30 μg of protein were loaded per lane. Proteins were separated on a 3% to 8% NuPage Tris-acetate polyacrylamide gel (Invitrogen) at 150 V for 1 h, and then transferred to nitrocellulose membranes by electrotransfer at 21 V for 18 h at 4°C.

Cypher/ZASP was detected using a 1:2,000 dilution of a mouse polyclonal anti-*Cypher/ZASP* antibody (28), followed by staining with horseradish peroxidase-labeled anti-mouse secondary antibody (Santa Cruz Biotechnology, Santa Cruz, California) and chemiluminescent detection using an enhanced chemiluminescence kit (Amersham-Biosciences).

RESULTS

Clinical evaluation. A total of 100 probands (69 Caucasian, 14 African-American, 13 Hispanic, 4 Asian) were

identified by standard clinical evaluation after presenting with features of heart failure (n = 91) or sudden death (n = 9). In all living cases, diagnostic criteria included a dilated left ventricular end-diastolic dimension and reduced systolic function using ejection fraction or fractional shortening measurements, with or without other features including trabeculation of the left ventricular myocardium consistent with INLVM, identified in 15 of the 100 probands (15%). All probands were classified as New York Heart Association (NYHA) functional class II to IV at the time of diagnosis. In all autopsy cases, evidence of left ventricular dilation, increased heart weight, and gross and anatomic features consistent with DCM or INLVM were used for diagnosis.

Evaluation of family history, as well as echocardiographic or MRI evaluation of relatives of the probands, identified 31 familial cases (defined as two or more affected individuals) and 69 sporadic cases. Creatine kinase levels were normal in all the probands or affected family members identified as mutation carriers, and there was no clinical evidence of skeletal myopathy.

Molecular analysis: genomic structure and sequences. Screening of a human BAC library identified two BACs (BAC 659G15 and BAC 656A18) containing most of the *Cypher/ZASP* coding sequence. Further alignments were performed by BLAST search, which identified two overlapping human genome clones from chromosome 10, namely RP11-41D8 and RP11-359E3 (GenBank accession numbers AL391985 and ACO67750, respectively), containing the entire *Cypher/ZASP* gene sequence.

The DNA sequence analysis identified 16 coding exons spanning approximately 70 kb (Fig. 1A) (Table 2). Six isoforms have been detected in human mRNA (Fig. 1A). The PDZ domain, which is present in all *Cypher/ZASP* isoforms, is encoded by exons 1 through 3, whereas exons 12 to 16 encode for the three LIM domains, which is shared by four of the six isoforms (Fig. 1A).

Mutation analysis. Mutations in *Cypher/ZASP* were identified in 6 (6%) of the 100 probands. Mutations were identified in two families (FDCM 066 and FDCM/INLVM 065) and four sporadic cases (DCM/INLVM 035, INLVM-11, INLVM-17, and DCM-31) (Figs. 2 to 5). None of these mutations were identified in 200 ethnically matched control individuals (400 chromosomes). The clinical characteristics of these patients and families are shown in Table 3.

All but one mutation identified in the *Cypher/ZASP* gene resulted in amino acid changes in residues that are conserved between different species, and all lie within the linker between the PDZ and LIM domains of the *Cypher/ZASP* protein (Fig. 1B). In addition, computer modeling of *Cypher/ZASP* wild-type and mutant proteins, using the PSIPRED V2.2 analysis software (32), predicted protein secondary structure changes in each of the mutated proteins (data not shown).

Familial DCM. FAMILY FDCM 066. An abnormal DHPLC pattern was identified in exon 10 of *Cypher/ZASP* (Fig. 2A).

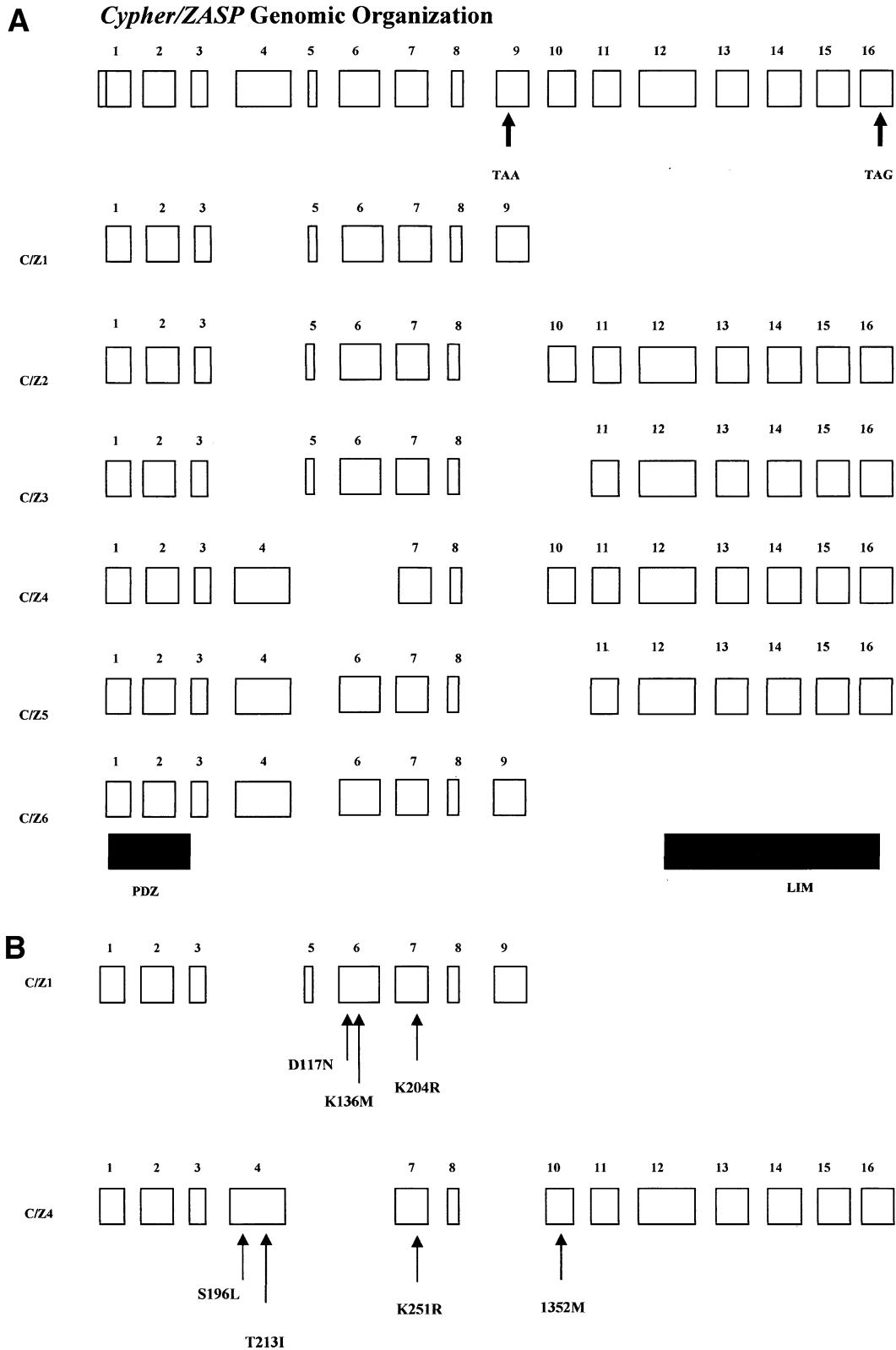


Figure 1. *Cypher/ZASP* genomic structure. (A) Representation of the *Cypher/ZASP* genomic structure (top), and six messenger ribonucleic acid isoforms, termed *Cypher/ZASP*-1, -2, -3, -4, -5, and -6. The PDZ domain is encoded by exons 1, 2, and 3; the three LIM domains are encoded by exons 12-16. (B) The location of mutations identified in this study. Note that the mutation in *C/Z1* will also be present in the *C/Z2* and 3 isoform (not shown), and the mutation in *C/Z4* will also be present in *C/Z5* and 6 isoform (not shown).

Table 2. Exon/Intron Boundaries in Human *Cypher/ZASP* Gene

Exon	Size	Splice Acceptor*	Splice Donor*†
1	172	...ttgtctgcagag GCGGCC	TCCCGG gtgagtgcacc... ..
2	152	...ctatccaatcag ATCACA	GCAGAA gtaggtgggagc... ..
3	76	...tggtttctacag ATCAAA	CAGAAG gtaggtgctgact... ..
4	368	...gcctgtgccag GACCCC	AGGAGG gtaggtaacgg... ..
5	23	...ttcctcccag GTGGTA	AGCCAA gttagtatcaa... ..
6	204	...ccctccccag CGCCGA	CAGTGG gtaagcctcc... ..
7	170	...tctgattacag GAGCCT	AATCA gtagtgcaggc... ..
8	37	...ttctaccacag TGCAAG	GTCAAG gtaagtgcctgg... ..
9	773	...tctgtccacag GGAAAG	AGCTAA
10	189	...cgcctcatcag CACCCC	CCCAAG gtaactgggcca... ..
11	146	...gcttggtccag GCCCCA	AGCCAG gtaagaggcaga... ..
12	445	...tggctttgcag TGCCTG	CATCCG gtaggtccagc... ..
13	181	...gtgctcccag GGGCC	ATGGGG gtaagtgggagg
14	121	...tcttccccag GAAGTA	AGAAAG gtaggaacactt... ..
15	116	...tttctattcag ACTACA	TGCGCA gtagtctcta... ..
16	2110	...tctctgtccag GTCTGC	TTGTAG

*Exonic sequences are shown in bold upper case while intronic sequences are in lower case: consensus splice site sequences are shown in bold. †For exons 9 and 16, the sequence at the termination codon is shown.

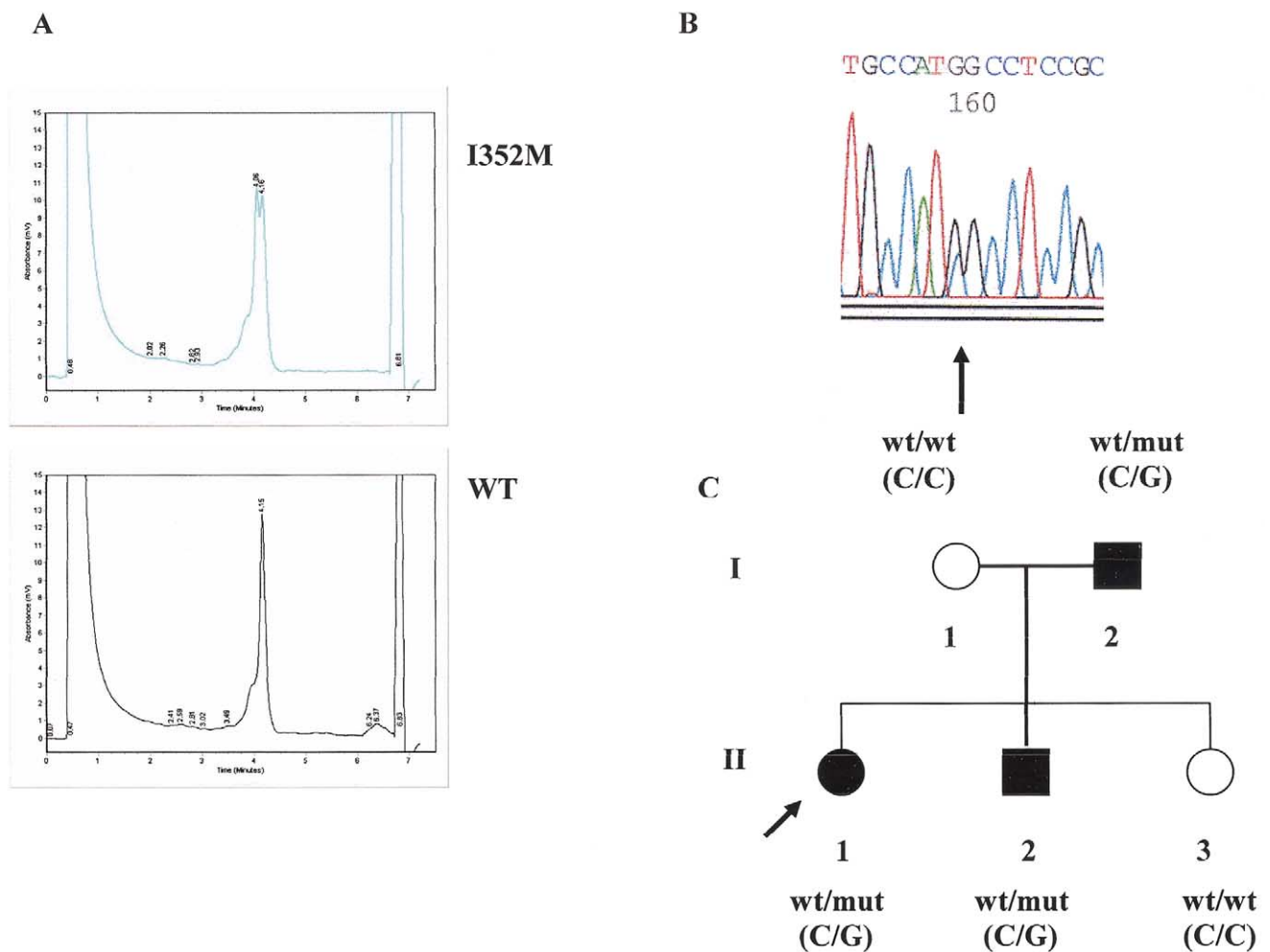


Figure 2. Mutation detection in FDCM 066. (A) Denaturing high performance liquid chromatography (DHPLC) of exon 10 identifies an abnormal DHPLC pattern in the proband (top panel) that is absent in controls (bottom panel). (B) The deoxyribonucleic acid (DNA) sequence analysis of genomic DNA identifies a C to G base substitution at position 1056. (C) Pedigree of family FDCM 066 showing the nucleotides identified at 1056. The arrow identifies the proband.

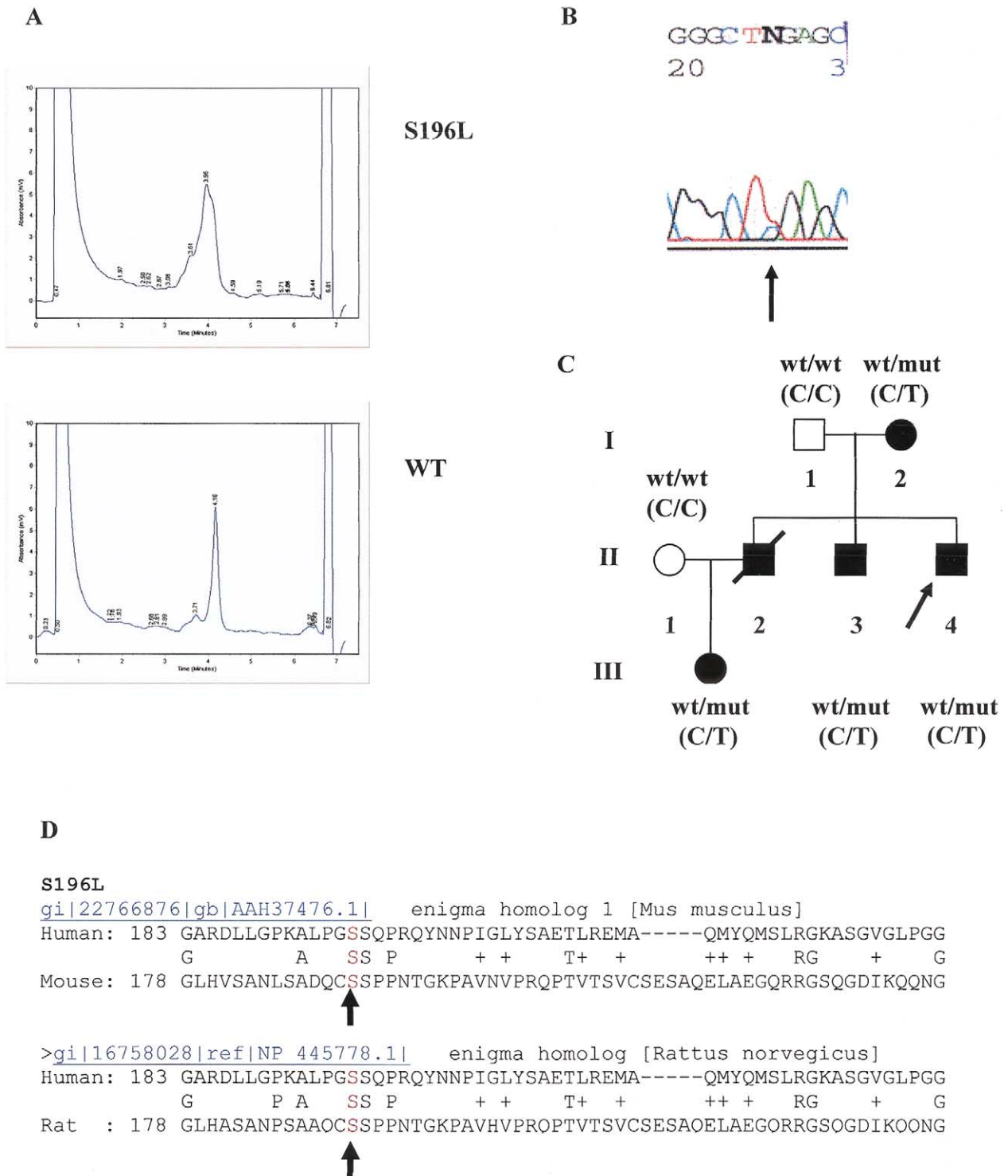


Figure 3. Mutation detection in FDCM/INLVM 065. **(A)** Denaturing high performance liquid chromatography (DHPLC) analysis of exon 4 identifies an abnormal DHPLC pattern in the proband (**top panel**) that is absent in controls (**bottom panel**). **(B)** The deoxyribonucleic acid (DNA) sequence analysis of genomic DNA identifies a C to T base substitution at position 587. **(C)** Pedigree of family FDCM/INLVM 065. The **arrow** identifies the proband. **(D)** Blast homology analysis of *Cypher/ZASP* amino acid sequence for residue S196.

The DNA sequence analysis identified a single nucleotide change, C1056G (Fig. 2B), which results in an amino acid change from isoleucine to methionine at position 352 (I352M) in *Cypher/ZASP4* (Fig. 1B). This amino acid

change is predicted to abolish an α -helix and a short β -sheet in *Cypher/ZASP* 4 (data not shown). This family has pure DCM and an inheritance pattern consistent with an autosomal dominant trait (Fig. 2C). Analysis of the

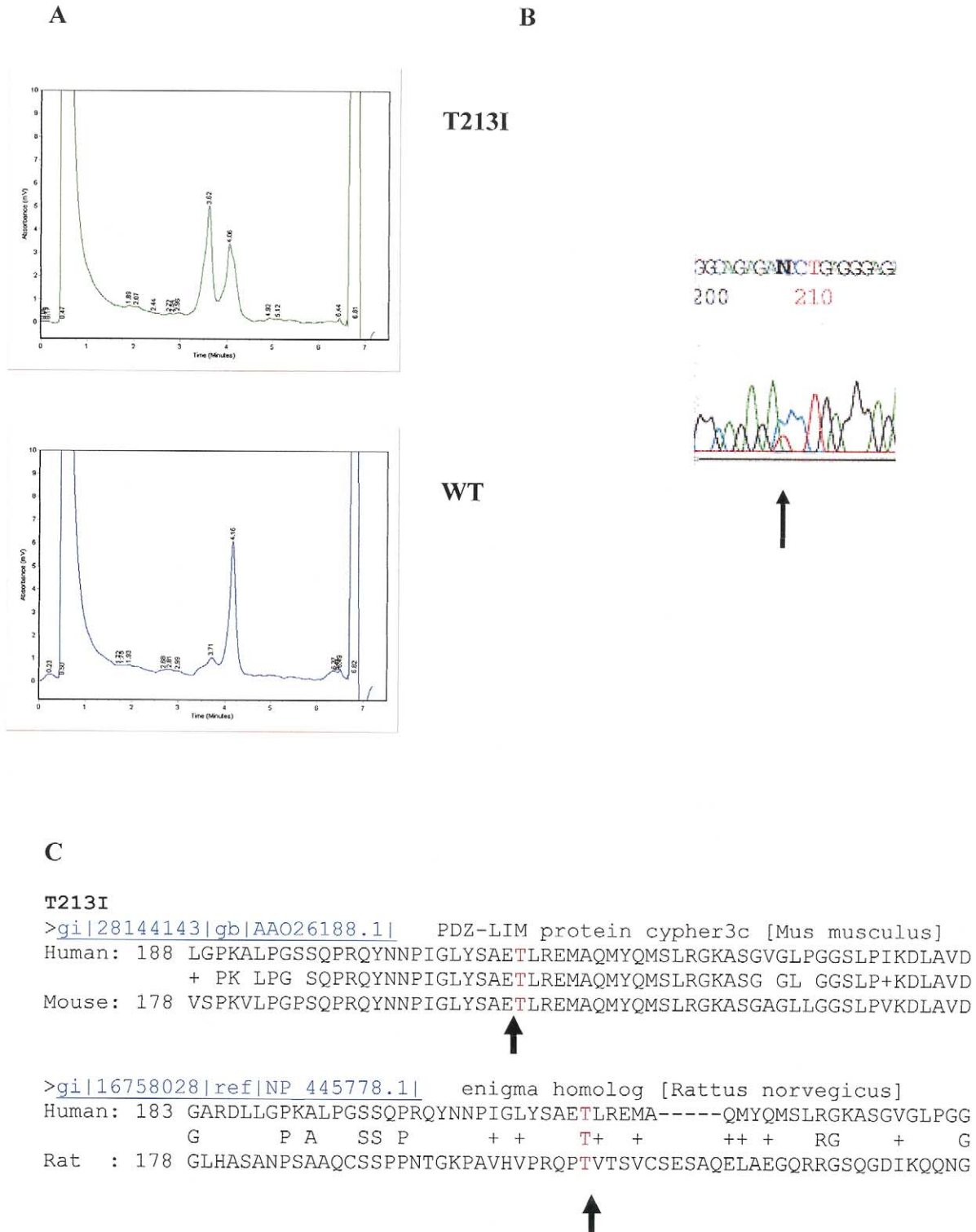


Figure 4. Mutation detection in DCM 035. (A) Denaturing high performance liquid chromatography (DHPLC) analysis of exon 4 identifies an abnormal DHPLC pattern (top panel), which is absent in controls (bottom panel). (B) The deoxyribonucleic acid (DNA) sequence analysis of genomic DNA identifies a C to T base substitution at position 638. (C) Blast homology analysis of *Cypher/ZASP* amino acid sequence for residue T213.

available family members showed that the affected individuals carried the same heterozygous mutation, while unaffected family members did not. This residue does not

appear to be highly conserved, although the variant we identified is not present in any species of *Cypher/ZASP* so far characterized.

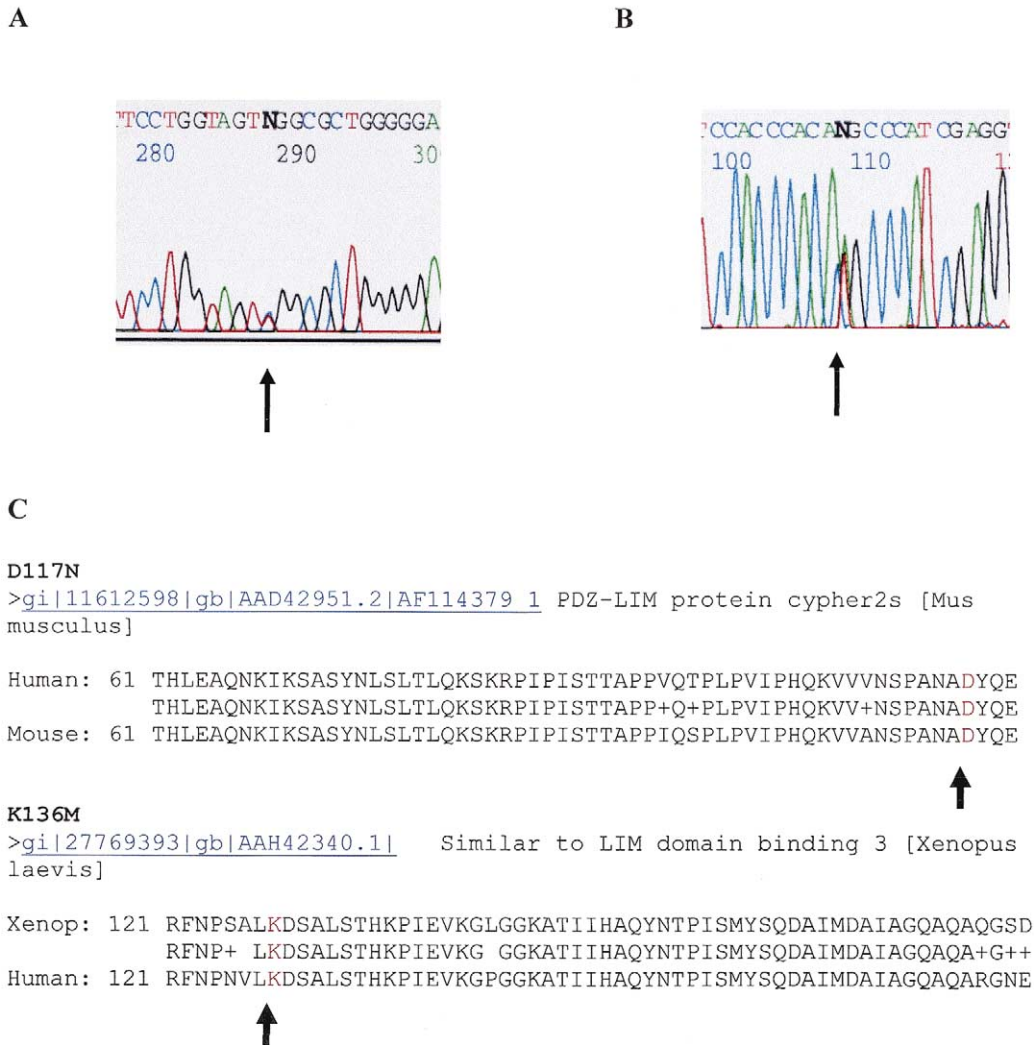


Figure 5. Mutations identified in INLVM-11, INLVM-17, and DCM-31. **(A)** The deoxyribonucleic acid (DNA) sequence analysis of exon 6 identifies a G349A substitution in Patient INLVM-11. Note that the reverse sequence is shown. **(B)** The DNA sequence analysis of genomic DNA from Patient DCM-31 identifies an A407T transversion. **(C)** Blast homology analysis of *Cypher/ZASP* amino acid sequence for residues D117 and K136.

FAMILY FDCM/INLVM 065. An abnormal DHPLC pattern was identified in exon 4 of the proband (Fig. 3A). The DNA sequence analysis identified a C587T missense mutation (Fig. 3B) that leads to the substitution of serine 196 with a leucine (S196L) in *Cypher/ZASP4* (Fig. 1B), resulting in the creation of a short α -helix beginning at residue 175 of *Cypher/ZASP4*, whereas the α -helix beginning at residue 214 is predicted to be abolished (data not shown). This residue is conserved in mouse and rat. The 40-year-old proband of this family was diagnosed with DCM associated with mild left ventricular hypertrophy and a trabeculated left ventricular on echocardiogram. In this family, there are four other affected individuals (Fig. 3C): individual I:2 is the mother of the proband (a 68-year-old); individuals II:2 and II:3 are the two brothers of the proband, one of which (II:2) died with a severe dilated cardiomyopathy at 41 years of age; and the living daughter (III:1) of the deceased brother, who is 7 years old and presented with a mildly dilated left

ventricle. The mutation was only identified in affected individuals; no DNA was available from the deceased subject.

Sporadic DCM and INLVM. PATIENT DCM/INLVM 035. This sporadic DCM patient, a 15-month-old Latin American male, was admitted to the hospital with profound bradycardia, atrioventricular block, premature ventricular contractions, monomorphic ventricular tachycardia, and depressed ventricular function with mild left ventricular dilation. During the subsequent three years of follow-up, the patient significantly improved by echocardiographic criteria, with only mild DCM currently noted. Screening of the parents demonstrated normal left ventricular size and function with no abnormalities on echocardiographic analysis.

An abnormal DHPLC pattern was identified in exon 4 (Fig. 4A), resulting in a C to T substitution of nucleotide 638 (Fig. 4B). This changed the amino acid at codon 213

Table 3. Clinical Findings in Patients With *Cypher/ZASP* Mutations

Family (#)	Subject	Mutation	Relation to Proband	Gender/Age	ECG	LVEDD (cm) (Z-Score)	FS%/EF% (Z-Score)	Dead	Neurologic Exam	CK-MM
FDCM-065	I:1	wt	Father	M/70 yrs	N1	5.20 (-0.60)	36/58 (1.05)	N	N1	<10
	I:2	S196L	Mother	F/68 yrs	Severe LVH	6.85 (4.95)	24/38 (-5.20)	N	N1	<10
	II:1	wt	Sister-in-law	F/40 yrs	N/A	N/A	N/A	N	N1	<10
	II:2	N/A	Brother	M/41 yrs	N/A	N/A	N/A	Y	N1	<10
	II:3	S196L	Brother	M/31 yrs	Severe LVH	7.27 (5.88)	28/43 (-4.40)	N	N1	<10
	II:4	S196L	Proband	M/40 yrs	Severe LVH	7.05 (5.10)	25/40 (-4.90)	N	N1	<10
FDCM-066	III:1	S196L	Niece	F/7 yrs	N/A	N/A	N/A	N	N1	<10
	I:1	wt	Mother	F/35 yrs	N1	4.25 (0.35)	35/54 (0.80)	N	N1	<10
	I:2	I352M	Father	M/35 yrs	LVH	6.99 (5.25)	18/31 (-7.50)	Y	N1	<10
	II:1	I352M	Proband	F/15 yrs	LVH	6.72 (7.65)	18/31 (-7.90)	Y	N1	<10
	II:2	I352M	Brother	M/17 yrs	LVH	6.81 (4.40)	20/33 (-6.90)	N	N1	<10
	II:3	wt	Sister	F/20 yrs	N1	4.05 (-0.90)	36/59 (1.16)	N	N1	<10
Sporadic-011		D117N	Proband	F/44 yrs	LBBB	5.9 (2.45)	23/40 (-4.30)	N	N1	<10
Sporadic-017		D117N	Proband	M/33 yrs	Severe LVH, IVCD, VB	5.6 (2.45)	24/42 (-4.10)	N	N1	<10
Sporadic-031		K136M	Proband	M/16 yrs	LVH	6.93 (4.77)	20/32 (-6.96)	N	N1	<10
Sporadic-035		T213I	Proband	M/15 months	Sinus Bradycardia, 2° AVB, PVC, VT (all resolved)	5.6 (6.30)	14/26 (-8.40)	No	N1	<10

ECG = electrocardiogram; EF = ejection fraction; FS = fractional shortening; LBBB = left bundle branch block; LVEDD = left ventricular end-diastolic dimension; LVH = left ventricular hypertrophy; N/A = not applicable; N1 = normal; wt = wild-type; Z-score = standard deviation.

from the polar amino acid threonine to the non-polar amino acid isoleucine (T213I) in *Cypher/ZASP4* (Fig. 1B), resulting in the creation of two short α -helices beginning at residues 291 and 343, while a short β -sheet was created at residue 352 (data not shown). Threonine 213 is conserved both in mouse and rat. Neither parent had this substitution. **PATIENTS INLVM-11 AND INLVM-17.** Abnormal DHPLC patterns were identified in exon 6 in the Caucasian patients INLVM-11 and INLVM-17. The INLVM-11 is a 44-year-old female, diagnosed at 41 years of age with sporadic form of DCM, NYHA functional class III heart failure, left bundle branch block on surface electrocardiogram, reduced systolic function (fractional shortening 23%), dilated left ventricular (5.9 cm), deep trabeculations, and reduced metabolic exercise testing, with a maximum oxygen consumption of 58% predicted at 14 ml/kg/min. She is now stabilized (NYHA functional class II) on angiotensin-converting enzyme inhibitor, beta-blocker, and diuretic therapy.

The INLVM-17 is a 33-year-old male, diagnosed with DCM at 30 years of age during a family echocardiographic screen after sudden death occurred within the family. Echocardiographic and MRI screening identified both left and right ventricular trabeculations, with an intraventricular conduction delay and ventricular bigeminy on electrocardiogram, as well as echocardiographic evidence of borderline systolic function and a dilated left ventricle. In the other family members, neither DCM nor INLVM was identified.

Sequence analysis identified a G349A mutation (Fig. 5A) in exon 6 of both patients, resulting in an amino acid change from the acidic aspartic acid to the neutral, polar asparagine at position 117 (D117N) in *Cypher/ZASP1*, -2, and -3 (Fig. 1B), and predicted to result in the suppression of four α -helices at residues 202, 229, 268, and 274, respectively (data not shown). Aspartic acid 117 is conserved in mouse and rat, while it is glutamic acid in *Xenopus laevis* and zebrafish.

PATIENT DCM-31. A further abnormal DHPLC pattern was identified in exon 6 in proband DCM-31, a 16-year-old Caucasian male referred to us from an outside institution and diagnosed with DCM by echocardiography. The DNA sequence analysis identified an A407T mutation (Fig. 5B) that changes the basic lysine to neutral, non-polar methionine at position 136 (K136M) in *Cypher/ZASP1*, -2, and -3 (Fig. 1B), and predicted to result in the loss of an α -helix at residue 202 and the creation of a α -helix at residue 246 (data not shown). The K136 residue is highly conserved in species ranging from human to *Xenopus laevis*.

The DNA was obtained from the parents, after informed consent, and the sequence analysis did not reveal the same change, consistent with a de novo mutation.

Genetic polymorphisms in DCM and INLVM. Another abnormal DHPLC pattern was identified in exon 7 in four probands with DCM, three Caucasians and one Asian, as well as one African-American proband with INLVM. The DNA sequence analysis identified an A612G mutation

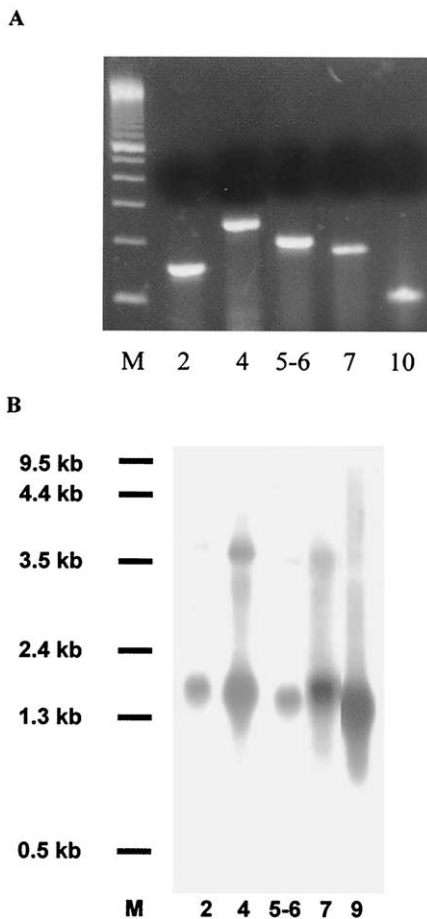


Figure 6. Analysis of the expression of *Cypher/ZASP* isoforms in human heart. The *Cypher/ZASP* exons were detected in human cardiac ribonucleic acid by reverse transcription-polymerase chain reaction (A) and Northern blot analysis (B). The exons identified are shown at the **bottom of each panel**. M = 100 bp deoxyribonucleic acid ladder (A). Positions of ribonucleic acid size markers are indicated (B).

(data not shown), which changes the basic amino acid lysine to the basic amino acid arginine at position 204 (K204R) in *Cypher/ZASP*1, -2, and -3 (position 251 in isoform 4 and position 319 in isoform 5 and 6) (Fig. 1B). This substitution was not found in 200 Caucasian, 200 Hispanic, and 200 Asian controls, but was identified in 6 of 100 African-American subjects, suggesting K204R is a modifier or polymorphism, rather than a disease-causing mutation.

Myocardial expression of *Cypher/ZASP*. We investigated the cardiac expression of each exon where *Cypher/ZASP* mutations were identified by RT-PCR and Northern blot analysis (Fig. 6). The detection of exons 2 and 7, present in all *Cypher/ZASP* isoforms, confirms that *Cypher/ZASP* is expressed in human heart. Exons 4 (C/Z4-6), 5 and 6 (C/Z1-3), and 10 (C/Z2 and 4) were detected (Fig. 6A), demonstrating the expression of these exons in human heart, and supporting a functional role of the mutations in cardiac disease. In addition, a strong signal was detected for exon 9 by Northern blot analysis of human cardiac RNA, suggesting a high expression of

isoforms C/Z1 and 6 (Fig. 6B). Sequencing analysis confirmed that the RT-PCR products were the expected *Cypher/ZASP* products.

***Cypher/ZASP* expression in transfected cells.** Expression of GFP following transient transfection of non-differentiated C2C12 cells with the pcDNA 3.1/NT-GFP-TOPO vector did not disrupt the actin cytoskeleton (Fig. 7A): GFP was distributed homogeneously throughout the cell (Fig. 7B). Expression of the wt-*Cypher/ZASP*-GFP fusion protein in non-differentiated C2C12s showed that *Cypher/ZASP* co-localizes with the intact actin cytoskeletal network (Figs. 7D to 7F). In contrast, in cells transfected with D117N-*Cypher/ZASP*, abnormal *Cypher/ZASP* and actin staining were observed, with disarray of the actin cytoskeleton in both (Figs. 7G to 7I).

Western blot analysis demonstrated that both wt-*Cypher/ZASP* and D117N-*Cypher/ZASP* were found exclusively in the insoluble fraction, and their expression levels were comparable (Fig. 8).

DISCUSSION

Over the last several years, the genetic basis of DCM has begun to be elucidated with the identification of several disease-causing genes. The mutant proteins have been shown to be involved in an apparent “final common pathway” (33), which links the extracellular matrix to the sarcolemma, sarcomere, and nuclear membrane. These genes include *dystrophin*, *G4.5*, *lamin A/C*, *desmin*, *actin*, *δ -sarcoglycan*, *β -sarcoglycan*, *β -myosin heavy chain*, *cardiac troponin T*, *α -tropomyosin*, *titin*, *vinculin*, *muscle LIM protein*, and *phospholamban* for “pure” DCM or conduction system disease associated with DCM (CDDC) (9,20-22). In addition, mutations in *α -dystrobrevin* and *G4.5* have been shown to cause DCM associated with INLVM (24).

Cypher/ZASP is a novel cardiac and skeletal muscle-specific Z-line protein (28) that is expressed in the cytoplasm, co-localizing with actin. The protein contains a PDZ domain that interacts with the C-terminus of *α -actinin-2* (28). The PDZ domain-containing proteins interact with each other in cytoskeletal assembly or with proteins involved in targeting and clustering of membrane proteins (34,35). A *Cypher* knockout mouse develops a severe congenital myopathy and dilated cardiomyopathy (36). Thus, we speculated that *Cypher/ZASP* could have an important role in the maintenance of the normal cytoarchitecture, and as such would be a candidate gene for DCM with or without other abnormalities, such as INLVM.

To assess the role of *Cypher/ZASP* in human cardiac diseases, we characterized the genomic structure of human *Cypher/ZASP*, identifying 16 coding exons and the exon-intron boundaries as well as the exon composition of each of the major isoforms.

Four major human *Cypher/ZASP* isoforms were originally described: *ZASP*, *ZASPV2*, *ZASPV3*, and *KIAA0613*-like (28). Here, we refer to the *ZASP*, *ZASPV3*, and *KIAA0613*-

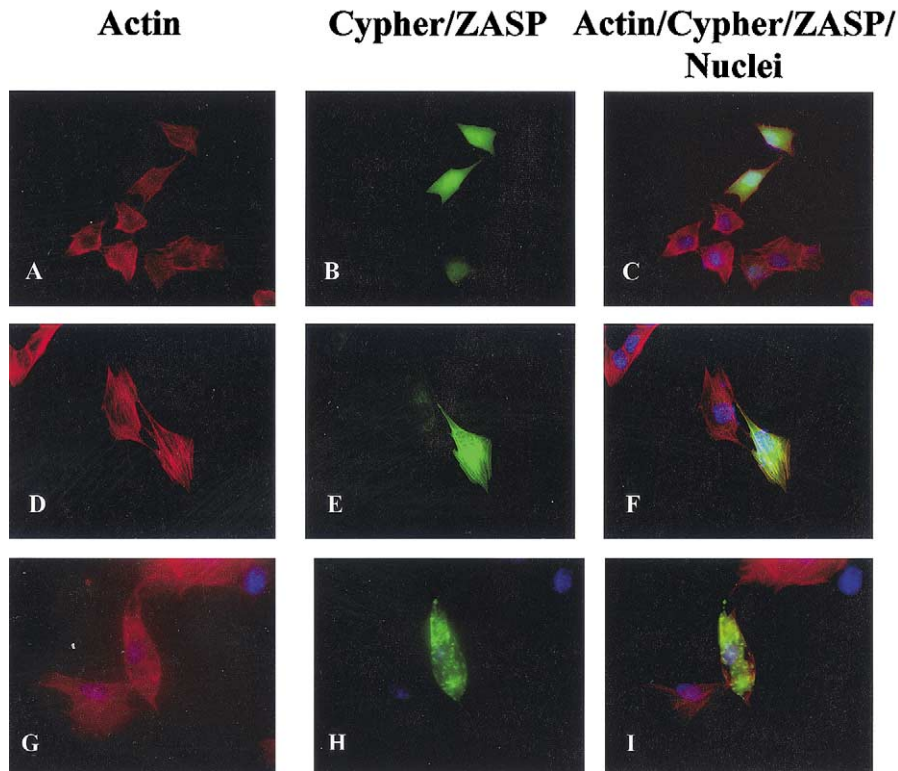


Figure 7. Immunohistochemical analysis of *Cypher/ZASP* expression. Immunohistochemical analysis of C2C12 cells transfected with the pcDNA3.1/NT-GFP-TOPO vector (A to C), or with constructs expressing wild type *Cypher/ZASP-1-GFP* (D-F) or D117N-*Cypher/ZASP-1-GFP* (G to I). Actin staining (red) is shown in the left panels, GFP (*Cypher/ZASP*) staining (green) is shown in the middle panels, while the right panels are the overlay of the ZASP, actin and DAPI (nuclei) images. All images were obtained using 40× magnification.

like variants as to *Cypher/ZASP1*, -3, and -4, respectively. In addition, three other isoforms have been identified in mice and humans. These are referred to as *Cypher/ZASP2*, -5, and -6 (Fig. 1A). We have been unable to identify the isoform *ZASPV2*.

The functional significance of the various isoforms is unknown, although their structure, either containing only the PDZ domain (*Cypher/ZASP1*) or containing both PDZ and LIM domains (*Cypher/ZASP2-5*), leads to the hypothesis of multiple functions, like other proteins that have similar domain arrangements, such as the muscle LIM protein (37).

We screened subjects with familial or sporadic forms of DCM, as well as patients with INLVM with hypertrophy,

dilation, and systolic dysfunction. We identified five *Cypher/ZASP* mutations in 6 of 100 probands screened (6% of cases), including two familial cases and four sporadic cases. None of the mutations were identified in 400 chromosomes from ethnic-matched controls, and all resulted in altered conserved amino acids, suggesting their functional importance.

In mice, isoforms containing exon 6 were highly expressed in skeletal muscle, but were not detectable in the heart by Western blot analysis (38). Here we have demonstrated that the domain encoded by exon 6 of human *Cypher/ZASP*, which encodes the D117N and K136M mutations, is expressed in human heart as detected by both Northern and Western blot analyses. Consistent with our results in humans, prolonged exposure times of both Northern and Western blots of extracts from mouse heart have revealed low levels of expression of *Cypher* isoforms containing exon 6 (Huang and Chen, personal communication, 2003). In addition, three of the *Cypher/ZASP* mutations are encoded by exons 4 (T213I, S196L) and 10 (I352M), which are present in *Cypher/ZASP2* and -4 isoforms whose expression in the human heart was previously unknown (28). Here we demonstrate that both exons 4 and 10 are expressed in the human heart, supporting the functional significance of these mutations in left ventricular dysfunction.

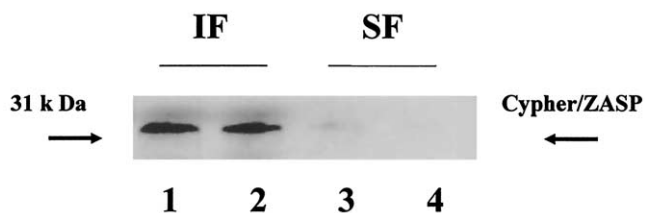


Figure 8. Western blot analysis of *ZASP* expression. Western blot analysis of protein isolated from C2C12 cells transfected with wild type (lanes 1 and 3), D117N (lanes 2 and 4) *Cypher/ZASP*, separated into insoluble (IF) and soluble (SF) fractions.

The I352M mutation was found in a family with “pure” DCM, where the proband and his offspring presented with typical DCM, but with phenotypic variability, while K136M was found in a sporadic DCM patient. However, the other mutations were found in individuals diagnosed with INLVM associated with left ventricular dilation and systolic dysfunction. Family 065, carrying the S196L mutation, showed a particularly malignant form in the mother and the brother of the proband, although the niece of the proband has a milder phenotype; however, this may be a function of age. The T213I mutation identified in sporadic case, DCM/INLVM 035, results in mild left ventricular dysfunction, but was associated initially with severe conduction disturbances, whereas the D117N mutation was associated with severe left ventricular dilation and the occurrence of particularly malignant rhythm abnormalities (Patients INLVM-11 and INLVM-17).

Although no phenotype-genotype correlation can be made at this stage of the study, it is interesting that mutations in exon 4 (S196L and T213I) lead to INLVM, suggesting a role for this domain in normal left ventricular morphogenesis and contractile function. Mutations D117N and K136M, encoded by exon 6, lead to INLVM and DCM, respectively, suggesting a more complex role for this domain. The mutation encoded by exon 10 (I352M) is associated with “pure” DCM in contrast to the other *Cypher/ZASP* mutations (S196L and T213I). Targeted protein-protein interaction analysis of these specific portions of *Cypher/ZASP* may explain the clinical heterogeneity.

At the time, complementary DNA clones of the exon 4 containing isoforms were not available and, therefore, our functional studies have been focused on the D117N mutation, encoded by exon 6. We hypothesized that expression of mutated *Cypher/ZASP* could affect the stability of actin cytoskeletal network, as well as its connection to the cell membrane. This was confirmed by the observation that in cells expressing the D117N mutation, the *Cypher/ZASP* mutation resulted in disarray of the actin cytoskeleton. We speculate that D117N affects *Cypher/ZASP* binding to proteins interacting with the actin network, such as α -actinin-2. Studies are underway to prove this hypothesis and to determine whether D117N alters the *Cypher/ZASP* secondary structure, thereby impairing the α -actinin-2 binding site, modifying *Cypher/ZASP* anchorage to the sarcomeric compartment, or whether it causes an indirect modification in the tertiary structure of the actin-binding site of α -actinin-2.

In conclusion, we have identified a new gene causing both the “pure” form of DCM and DCM associated with INLVM. This gene, *Cypher/ZASP*, encodes a specific Z-line PDZ-domain protein, playing a potential important role in bridging the sarcomere to the cytoskeletal network. Description of multiple mutations in *Cypher/ZASP* in patients with DCM and INLVM suggests that disruption of this gene is a common cause of left ventricular dysfunction and dilation, and it provides further support for the concept

that disruption of the cytoarchitecture, comprising the cytoskeleton, sarcolemma, sarcomere, and interacting components is pivotal to the development of left ventricular dysfunction. Although all the patients with *Cypher/ZASP* mutation had normal creatine kinase levels and muscle function, mutations that were identified in *Cypher/ZASP* isoforms and expressed in skeletal muscle leads to the possibility that *Cypher/ZASP* mutations are responsible for skeletal muscle abnormalities associated with heart failure (such as fatigue and exercise intolerance), as has been described for patients with β - and δ -sarcoglycan, *dystrophin*, *G4.5*, *desmin*, and *lamin A/C mutations* (9,39). The common frequency of mutations in this gene and its interactions with other proteins of the actin cytoskeleton shown to cause left ventricular dysfunction suggest that this component of the heart and skeletal muscle is important in functional integrity.

Acknowledgments

The authors are grateful to Dr. Paolo Vatta for useful discussions and Melba Koegele for administrative support.

Reprint requests and correspondence: Dr. Jeffrey A. Towbin, Pediatric Cardiology, Texas Children’s Hospital, 6621 Fannin Street, F.C. 430.09, Houston, Texas 77030. E-mail: jtowbin@bcm.tmc.edu.

REFERENCES

1. Dec GW, Fuster V. Idiopathic dilated cardiomyopathy. *N Engl J Med* 1994;331:1564–75.
2. Codd MB, Sugrue DD, Gersh BJ, Melton LJ 3rd. Epidemiology of idiopathic dilated and hypertrophic cardiomyopathy: a population-based study in Olmsted County, Minnesota, 1975 to 1984. *Circulation* 1989;80:564–72.
3. Manolio TA, Baughman KL, Rodeheffer R, et al. Prevalence and etiology of idiopathic dilated cardiomyopathy. *Am J Cardiol* 1992;69:1458–66.
4. Kasper EK, Agema WR, Hutchins GM, Deckers JW, Hare JM, Baughman KL. The causes of dilated cardiomyopathy: a clinicopathologic review of 673 consecutive patients. *J Am Coll Cardiol* 1994;23:586–90.
5. Towbin JA. Pediatric myocardial disease. *Pediatr Clin North Am* 1999;46:289–312.
6. Michels VV, Moll PP, Miller FA, et al. The frequency of familial dilated cardiomyopathy in a series of patients with idiopathic dilated cardiomyopathy. *N Engl J Med* 1992;326:77–82.
7. Keeling PJ, Gang Y, Smith G, et al. Familial dilated cardiomyopathy in the United Kingdom. *Br Heart J* 1995;73:417–21.
8. Grunig E, Tasman JA, Kucherer H, Franz W, Kubler W, Katus HA. Frequency and phenotypes of familial dilated cardiomyopathy. *J Am Coll Cardiol* 1998;31:186–94.
9. Towbin JA, Bowles NE. The failing heart. *Nature* 2002;415:227–33.
10. Olson TM, Michels VV, Thibodeau SN, Tai YS, Keating MT. Actin mutations in dilated cardiomyopathy, a heritable form of heart failure. *Science* 1998;280:750–2.
11. Li D, Tapscoft T, Gonzalez O, et al. Desmin mutation responsible for idiopathic dilated cardiomyopathy. *Circulation* 1999;100:461–4.
12. Fatkin D, MacRae C, Sasaki T, et al. Missense mutations in the rod domain of the lamin A/C gene as causes of dilated cardiomyopathy and conduction-system disease. *N Engl J Med* 1999;341:1715–24.
13. Tsubata S, Bowles KR, Vatta M, et al. Mutations in the human delta-sarcoglycan gene in familial and sporadic dilated cardiomyopathy. *J Clin Invest* 2000;106:655–62.

14. Barresi R, Di Blasi C, Negri T, et al. Disruption of heart sarcoglycan complex and severe cardiomyopathy caused by beta sarcoglycan mutations. *J Med Genet* 2000;37:102–7.
15. Kamisago M, Sharma SD, DePalma SR, et al. Mutations in sarcomere protein genes as a cause of dilated cardiomyopathy. *N Engl J Med* 2000;343:1688–96.
16. Olson TM, Kishimoto NY, Whitby FG, Michels VV. Mutations that alter the surface charge of alpha-tropomyosin are associated with dilated cardiomyopathy. *J Mol Cell Cardiol* 2001;33:723–32.
17. Gerul IB, Gramlich M, Atherton J, et al. Mutations of TTN, encoding the giant muscle filament titin, cause familial dilated cardiomyopathy. *Nat Genet* 2002;30:201–4.
18. Itoh-Satoh M, Hayashi T, Nishi H, et al. Titin mutations as the molecular basis for dilated cardiomyopathy. *Biochem Biophys Res Commun* 2002;291:385–93.
19. Olson TM, Illenberger S, Kishimoto NY, Huttelmaier S, Keating MT, Jockusch BM. Metavinculin mutations alter actin interaction in dilated cardiomyopathy. *Circulation* 2002;105:431–7.
20. Knoll R, Hoshijima M, Hoffman HM, et al. The cardiac mechanical stretch sensor machinery involves a Z disc complex that is defective in a subset of human dilated cardiomyopathy. *Cell* 2002;111:943–55.
21. Haghighi K, Kolokathis F, Pater L, et al. Human phospholamban null results in lethal dilated cardiomyopathy revealing a critical difference between mouse and human. *J Clin Invest* 2003;111:869–76.
22. Schmitt JP, Kamisago M, Asahi M, et al. Dilated cardiomyopathy and heart failure caused by a mutation in phospholamban. *Science* 2003;299:1410–3.
23. Bione S, D'Adamo P, Maestrini E, Gedeon AK, Bolhuis PA, Toniolo D. A novel X-linked gene, G4.5 is responsible for Barth syndrome. *Nat Genet* 1996;12:385–9.
24. Ichida F, Tsubata S, Bowles KR, et al. Novel gene mutations in patients with left ventricular non-compaction or Barth syndrome. *Circulation* 2001;103:1256–63.
25. Chin TK, Perloff JK, Williams RG, Jue K, Mohrmann R. Isolated non-compaction of left ventricular myocardium: a study of eight cases. *Circulation* 1990;82:507–13.
26. Towbin JA, Bowles NE. Sarcoglycan, the heart, and skeletal muscles: new treatment, old drug? *J Clin Invest* 2001;107:107–8.
27. Zhou Q, Ruiz-Lozano P, Martone ME, Chen J. Cypher, a striated muscle-restricted PDZ and LIM domain-containing protein, binds to alpha-actinin-2 and protein kinase C. *J Biol Chem* 1999;274:19807–13.
28. Faulkner G, Pallavicini A, Formentin E, et al. ZASP: a new Z-band alternatively spliced PDZ-motif protein. *J Cell Biol* 1999;146:465–75.
29. Bowles KR, Abraham SE, Brugada R, et al. Construction of a high-resolution physical map of the chromosome 10q22-q23 dilated cardiomyopathy locus and analysis of candidate genes. *Genomics* 2000;67:109–27.
30. Pauschinger M, Bowles NE, Fuentes-Garcia FJ, et al. Detection of adenoviral genome in the myocardium of adult patients with idiopathic left ventricular dysfunction. *Circulation* 1999;99:1348–54.
31. Vatta M, Stetson SJ, Perez-Verdia A, et al. Molecular remodeling of dystrophin in patients with end-stage cardiomyopathies and reversal in patients on assistance-device therapy. *Lancet* 2002;359:936–41.
32. McGuffin LJ, Bryson K, Jones DT. The PSIPRED protein structure prediction server. *Bioinformatics* 2000;16:404–5.
33. Bowles NE, Bowles KR, Towbin JA. The “final common pathway” hypothesis and inherited cardiovascular disease: the role of cytoskeletal proteins in dilated cardiomyopathy. *Herz* 2000M;25:168–75.
34. Craven SE, Bredt DS. PDZ proteins organize synaptic signaling pathways. *Cell* 1998;93:495–8.
35. Fanning AS, Anderson JM. PDZ domains: fundamental building blocks in the organization of protein complexes at the plasma membrane. *J Clin Invest* 1999;103:767–72.
36. Zhou Q, Chu PH, Huang C, et al. Ablation of Cypher, a PDZ-LIM domain Z-line protein, causes a severe form of congenital myopathy. *J Cell Biol* 2001;155:605–12.
37. Arber S, Hunter JJ, Ross J, Jr., et al. MLP-deficient mice exhibit a disruption of cardiac cytoarchitectural organization, dilated cardiomyopathy, and heart failure. *Cell* 1997;88:393–403.
38. Huang C, Zhou Q, Liang P, et al. Characterization and in vivo functional analysis of splice variants of Cypher. *J Biol Chem* 2003;278:7360–5.
39. Towbin JA. The role of cytoskeletal proteins in cardiomyopathies. *Curr Opin Cell Biol* 1998;10:1319.